

High ALDH^{dim}-expressing CD34⁺CD38⁻ cells in leukapheresed peripheral blood is a reliable guide for a successful leukemic xenograft model of acute myeloid leukemia

JI YOON LEE^{1*}, SOHYE PARK^{1*}, A-REUM HAN¹, JIHYANG LIM², WOO-SUNG MIN¹ and HEE-JE KIM¹

¹Cancer Research Institute, Department of Hematology, Catholic Blood and Marrow Transplantation Center, College of Medicine, The Catholic University of Korea;

²Laboratory Medicine, The Catholic University of Korea, Seoul, Republic of Korea

Received May 8, 2014; Accepted July 9, 2014

DOI: 10.3892/or.2014.3359

Abstract. The primary human acute myeloid leukemia (AML) cell injection xenograft mouse model is used to investigate multimodal therapies and drug screening on tumor growth. Since xenograft models using human cell lines to examine drug response are not correlated with the clinical outcomes observed in patients, a xenograft model using primary human cells has been used as a more appropriate model with which to minimize this problem. Although bone marrow (BM) cells from patients are often regarded as superior sources to establish xenograft models due to the high frequency of stem cell populations, there is a fatal drawback; only small volumes can be obtained and used for the generation of the leukemic xenograft model. Indeed, longevity of AML characteristics, as well as sufficient stem cells in the xenograft model, should be guaranteed to analyze the therapeutic response to a drug. Therefore, we examined whether leukapheresed peripheral blood (LPB) consists of reliable leukemic stem cells (LSCs) and ALDH^{dim}-expressing CD34⁺CD38⁻ cells, and functions in grafting human AML with virulence compared to that of BM. LPB cells showed an advantage for the xenograft mouse model with AML cell homing, engraftment and a high human ALDH^{dim}-expressing CD34⁺CD38⁻ cell population, suggesting an alternative cell source to BM. Overall, this xenograft model using LPB offers the possibility of overcoming the small volume limitation of BM and prevents individual variation by

using a single LPB sample. This result is noteworthy in identifying cell sources capable of generating a stable xenograft model.

Introduction

Acute myeloid leukemia (AML) is morphologically defined by an abnormal increase in myeloblasts in the bone marrow (BM). Since AML is heterogeneous in regards to morphologic and cytogenetic features, patient prognoses are extremely variable. To improve understanding of the biological features of human AML, several mouse models have been developed, including a xenograft model and a genetically engineered mouse model (1,2). The xenograft model has been shown to better mimic the therapeutic responses and tumor microenvironment observed in the human condition, as well as being rapidly produced within several weeks (3). The xenograft model of leukemic progression in human beings has been gradually improved. Successful transplantation of human hematopoietic cells into immunodeficient mice was first reported in studies from the late 1980s that used homozygous severe combined immunodeficient (C.B.17-SCID) mice (4,5). Then, modified SCID model studies showed that, irrespective of the morphologic subtypes, only a small fraction of leukemic cells, the putative leukemic stem cells (LSCs), could recapitulate leukemia (6-8). Among the many types of mouse strains used for the xenograft model, the most advanced strain is the nonobese diabetic, severe combined immunodeficiency (NOD/SCID) mouse with targeted deletion of the interleukin (IL-2) receptor with the common γ -chain (IL-2R γ^{null}), termed the NSG mouse. This mouse has a stable lack of mature T, B and NK cells, a prolonged survival beyond 16 months of age and is acceptable for engraftment of primary human cells. Ishikawa *et al* showed the efficient development of functional human hemato-lymphopoiesis in the NOD/SCID/IL2 γ^{null} newborn model (9). After these reports, he continuously demonstrated that LSCs exclusively recapitulate AML and retain self-renewal capacity *in vivo* (10), suggesting the importance of LSCs. Because other immunodeficient mice have a short life-span and a disturbed long-term evaluation in *in vivo* studies, NSG mice were used to establish a leukemic xenograft

Correspondence to: Professor Hee-Je Kim, Division of Hematology, Department of Internal Medicine, Catholic Blood and Marrow Transplantation Center, Seoul St. Mary's Hospital, College of Medicine, The Catholic University of Korea, 505 Banpo 4-dong, Seocho-gu, Seoul 137-701, Republic of Korea
E-mail: cumckim@catholic.ac.kr

*Contributed equally

Key words: leukapheresed peripheral blood, leukemic xenograft, CD34⁺CD38⁻ cells, ALDH^{dim} cells

model with long-term survival. Although many investigators have reported established mouse models using mononuclear cells (MNCs), such models have shown low rates of success due to individual variation in LSC potential. Therefore, some scientists often decide to use BM-MNCs equivalent to more than 10,000 LSCs after calculation in a xenograft model (11,12). CD34⁺CD38⁻ cells, known as LSCs, are the main cell population responsible for producing leukemia due to their self-renewing properties (13). Lapidot *et al* reported that AML cells with the CD34⁺CD38⁻ phenotype are capable of producing leukemia in immunodeficient mice (14). Although the identification of functional LSCs is still debated, CD34⁺CD38⁻ are currently accepted as representative markers for LSCs *in vivo* as well as *in vitro* (13,15). Recently, the capacity of aldehyde dehydrogenase dim (ALDH^{dim})-positive cells to repopulate following injection into NSG mice with leukemic properties was addressed by Gerber *et al* (16). Hence, ALDH^{dim} cells in leukapheresed peripheral blood (LPB) that are also CD34⁺CD38⁻ were the main focus in the present study, and we investigated whether LPB from AML patients possesses a high level of LSCs with an abundant ALDH^{dim} population compared to that of the BM counterpart. We found that LPB, which displayed a high proportion of ALDH^{dim}-expressing CD34⁺CD38⁻ cells, contributes as much as BM to establishing a leukemic xenograft model repetitively and can be used as an alternative cell source without having the limitations of volume and a short life-span. Collectively, this study is the first to report the comparison between using BM and LPB cells in a leukemic xenograft model and provides beneficial information for investigators who attempt the xenograft model using primary leukemic cells.

Materials and methods

Human primary cells and cell lines. All experiments were performed with authorization from the Institutional Review Board for Human Research at the Catholic University of Korea. AML blood samples were obtained from the Catholic Blood and Marrow Transplantation Center at Seoul St. Mary's Hospital. A total of 16 AML samples were prospectively collected and examined. Samples were obtained from both newly diagnosed and relapsed patients. These patients showed diverse FAB subtypes, including M0 (1 case), M1 (2 cases), M2 (3 cases), M3 (1 case), M4 (5 cases) and M5 (4 cases). BM and LPB samples were frozen in fetal bovine serum with 10% DMSO and stored in liquid nitrogen. BM-derived mononuclear cells (BM-MNCs) and PB-derived MNCs (PB-MNCs) were fractionated by density gradient centrifugation using Ficoll-Paque™ Plus (17-1440-03; GE Healthcare Life Sciences, Piscataway, NJ, USA). The clinical characteristics and experimental information of the AML patients enrolled in the present study are listed in Table I. The cell lines TF-1a, K562 and Kasumi-6 were originally obtained from the American Type Culture Collection (ATCC, Rockville, MD, USA). These cells were grown in the appropriate culture media recommended by the ATCC.

Mice and human xenograft model. All mice were bred by the Department of Laboratory Animal at the Catholic University of Korea. NOD/ShiLtSz-*scid*/IL2R^γ^{null} (NOD.

Cg-Prkdc^{scid}Il2rg^{tm1Wjl}/SzJ, termed NSG) mice were purchased from the Jackson Laboratory and housed in ventilated micro-isolator cages in a high-barrier facility under specific pathogen-free conditions. Autoclaved water and irradiated food were provided *ad libitum*. All protocols for animal experiments were approved by the Institutional Animal Care and Use Committee of the Catholic University of Korea. For the xenograft model, 8-week-old mice were sublethally irradiated with 300 cGy of total body irradiation 24 h before intravenous injection of leukemic cells. AML blood samples were thawed at 37°C, washed twice in PBS, and cleared of aggregates and debris using a 40-μm cell filter. For the i.v. injection, cells were suspended in PBS at a final concentration of 1x10⁷ cells per 200 ml of PBS per mouse. Mice were monitored daily for symptoms of disease, including ruffled coat, hunched back, weakness and reduced motility. Once injected animals showed signs of distress, they were sacrificed. If no signs of stress were observed, mice were analyzed at 15 weeks following transplantation. The time from transplantation to sacrifice varied from 8 to 15 weeks with an average of 10 weeks.

Gross examination and survival monitoring. After injection, mice were sacrificed at signs of sickness and observed for tumor burden, characterized by tumor cluster in liver, suppression of erythropoiesis in BM and enlarged spleen. Femur (BM), spleen, and blood from NSG mice were collected and analyzed for lodgments of leukemia cells.

PCR and DNA fingerprinting. Total RNA isolation and DNA synthesis were performed as previously described (17). Human MLL/AF9 primers (forward, 5'-aatagaggaggcagccgaag-3' and reverse, 5'-gtccagcgagcaaatgata-3') were used. PCR work for fingerprinting was performed using a universal fingerprinting kit (JK Biotech Korea, cat no. JK090016) according to the manufacturer's protocol. UPF 2, 5, 13 primers were used to confirm origination, and PCR reactions were performed in a 50-μl PCR mixture containing 100 ng of each primer, 1X TE buffer, 100 ng of template DNA, 2.5 units HQ *Taq* polymerase and 2.5 mM of dNTP. PCR amplification was performed in a conventional PCR machine (Px2 Thermal Cycler; Thermo Electron Corp., Marietta, OH, USA) using the following profile: one cycle of 4 min at 94°C; 38 cycles of 1 min at 94°C, 1 min at 55°C, and 2 min at 72°C; one final extension cycle of 7 min at 72°C. PCR products were electrophoresed in a 2.0% agarose gel at 12 V/cm with TAE buffer. DNA fragments in the gel were visualized by staining with ethidium bromide and photographed under a UV transilluminator.

Flow cytometry. FACS staining and analysis of MNCs were performed as previously described (18). Briefly, cells were resuspended in 100 μl of rinsing buffer and incubated with antibodies. After washing, the cells were analyzed using a FACSCalibur flow cytometer equipped with Cell Quest® software (BD Biosciences, San Diego, CA, USA). We used phycoerythrin (PE)-conjugated mouse anti-human CD34 and PEcy5-conjugated mouse anti-human CD38 primary antibodies (555822 and 555461, respectively; both from BD Pharmingen) to examine LSCs. For engraftments, FITC-conjugated mouse anti-human CD45 and allophycocyanin (APC)-conjugated rat anti-mouse CD45 (555482 and 559864 respectively, both

Table I. Clinical and laboratory features of the AML patients.

Patients	FAB subtype	Age (years)	Gender	Cell source	WBCs/mm ³ at diagnosis	Cytogenetic anomalies	Molecular defects
1	M5b	56	F	PB	147,800	46,XY[20]	Negative
2	M4	56	F	PB	18,510	46,XX,add(12)(p13),der(16)inv(16)(p13.1q22)del(16)(q22)[28]/46,XX[2]	CBFb/MYH11
3	M4	58	M	PB	40,800	46,XY[20]	Negative
4	M2	15	F	PB	15,310	46,XX[20]	Negative
5	M1	58	M	PB	15,300	46,XY[20]	Negative
6	M5	27	M	PB	149,550	46,XY[20]	Negative
7	M4	41	F	PB	4,970	46,XX,inv(3)(q21q26.3)[20]	Negative
8	M1	27	M	PB	2,150	46,XY,t(9;11)(p22;q23)[26]/46,idem,add(1)(p36.1)[4]	MLL/AF9
9	M3	45	M	PB	2,400	46,XY[20]	Negative
10	M4	63	F	PB	35,370	46,XX[19]	Negative
11	M1	17	M	PB	18,230	45,X,-Y,t(8;21)(q22;q22)[6]/46,XY[14]	AML1/ETO
12	M1	45	F	PB	8,000	48,XX,+8,+10[25]/46,XX[5]	Negative
13	M2	27	M	PB	11,560	46,XY,del(9)(q22q31),del(11)(q13q23)[22]/46,XY[8]	Negative
14	M4	28	F	PB	30,900	46,XX,inv(16)(p13.1q22)[20]	CBFb/MYH11
15	M1	39	M	PB	10,700	46,XY,t(10;11)(q22;q23)[10]/47,idem,+21[30]	Negative
16	AML from ET	73	M	PB	20,120	47,XY,+8[20]	Negative
17	M2	50	F	PB	1,200	46,XX,t(11;17)(q23;q21)[22]/46,XX[3]	Negative
18	M2	63	F	PB	1,240	46,XX[20]	Negative
19	M2	34	F	PB	6,860	46,XX,del(2)(q33),add(5)(q31),del(6)(p23),del(7)(q32),t(8;21)(q22;q22),add(10)(q26),add(11)(p15),t(?11;12)(q21;p13)[cp17]/46,XX[3]	Negative
20	M1	34	M	BM	28,180	46,X,idic(Y)(q12)x2,dup(1)(q12q42),-16,der(21)t(16;21)(p11.2;q22)[7]/47,idem,+idic(Y)[13]	TLS/ERG
21	M2	49	M	BM	4,500	46,XY,t(1;11)(q21;q23)[20]	MLL/AF1q
22	M1	19	M	BM	139,610	46,XY,inv(16)(p13.1q22)[20]	CBFb/MYH11
23	M3	56	F	BM	11,650	45,XX,add(3q),del(17q),-18	Negative
24	M5b	15	F	BM	302,010	48,XX,+8,+13[7]/48,idem,del(13)(q12q14)[17]/52,idem,+4,+8,+10,+13[5]/46,XX[1]	Negative
25	M5	51	F	BM	45,790	46,XY[20]	Negative
26	M4	50	F	BM	52,920	47,XX,+add(1)(p13)[10]/46,XX[10]	Negative
27	M4	56	F	BM	18,510	46,XX,add(12)(p13),der(16)inv(16)(p13.1q22)del(16)(q22)[28]/46,XX[2]	CBFb/MYH11
28	M2	15	F	BM	15,310	46,XX[20]	Negative
29	M7	27	M	BM	239,400	47,XY+8[17]/46,XY[5]	Negative
30	M4	50	F	BM	195,280	46,XX[20]	Negative
31	M3	45	M	BM	2,400	46,XY[20]	Negative
32	M5	27	M	BM	149,550	46,XY[20]	Negative
33	M4	43	M	BM	1,920	46,XY[20]	Negative
34	M5	27	M	BM	2,150	46,XY,t(9;11)(p22;q23)[26]/46,idem,add(1)(p36.1)[4]	MLL/AF9
35	M3	41	M	LPB	43,010	46,XY,t(15;17)(q22;q12)[20]	PML/RARA
36	M3	46	M	LPB	31,770	46,XY,t(15;17)(q22;q21)[20]	AML M3 PML/RARa(+) F(TKD+)NC(-)
37	M2	17	M	LPB	120,160	46,XY[20]	Negative
38	M3	60	F	LPB	83,650	46,XX,t(15;17)(q22;q12)[20]	Negative
39	MRC	17	M	LPB	115,970	6,XY,der(9)del(p13p22)inv(p12q13)[18]/46,XY[2]	Negative
40	M1	52	F	LPB	100,250	46,XX[20]	Negative

Table I. Continued.

Patients	FAB subtype	Age (years)	Gender	Cell source	WBCs/mm ³ at diagnosis	Cytogenetic anomalies	Molecular defects
41	M4	53	M	LPB	13,800	46,XY[20]	Negative
42	M1	31	M	LPB	138,940	46,XY[20]	Negative
43	M2	58	M	LPB	145,690	46,XX[20]	Negative
44	M2	27	M	LPB	30,090	46,XX,t(9;11)(p22;q23)[20]	MLL/AF9
45	M4	45	M	LPB	218,610	47,XY,+mar[3]/46,XY[22]	Negative
46	M5b	60	F	LPB	143,720	46,XX,t(6;11)(q27;q23)[20]	Negative
47	M0	57	M	LPB/BM	4,390	46,XX[20]	Negative
48	M4	58	M	LPB/BM	142,700	46,XX,t(6;11)(q27;q23)[30]	MLL/AF6
49	M2	58	M	LPB	13,530	46,XY[20]	Negative
50	M4	58	M	LPB	23,140	46,XY[20]	Negative
51	M4e	15	F	LPB	154,500	46,XY,t(9;22)(q34;q11.2).inv(16)(p13.1q22)[13]/47,idem,+17[15]/48,idem,+8,+17[2]	Negative

F, female; M, male; AML, acute myeloid leukemia; FAB, French American British; WBCs, white blood cells; PB, peripheral blood; LPB, leukapheresed peripheral blood; BM, bone marrow.

from BD Pharmingen) were used. For secondary Abs, proper isotype-matched IgG and unstained controls were used to detect primary signals. ALDH activity was measured in MNCs according to the manufacturer's instructions (Aldefluor™; StemCo Biomedical Inc., San Diego, CA, USA).

Histology. BM samples were fixed in PFA, decalcified with 5% formic acid and embedded in paraffin. Prepared slides were counterstained with Meyer's hematoxylin. Hematoxylin and eosin (H&E) staining was used after fixation to confirm leukemic blast infiltration in BM.

Statistical analysis. Results are presented as the means ± SE. Data were compared using the Mann-Whitney U test. GraphPad Prism® software, ver. 4 (GraphPad software, La Jolla, CA, USA) was used for analyses. Values of $P < 0.05$ were considered to indicate statistically significant differences.

Results

LPB in AML patients shows a high level of leukemic stem cells, CD34⁺CD38⁻ cells. We investigated whether a difference in the frequency of CD34⁺CD38⁻ cells exists between PB, LPB and BM samples. AML is propagated by self-renewing leukemic stem cells characterized by the CD34⁺CD38⁻ phenotype. FACS analysis was performed using PB, LPB and BM samples from patients and the cell lines TF-1a, K562 and Kasumi-6. No significant difference in the proportion of CD34⁺CD38⁻ cells was detected in PB, LPB and BM (PB, 5.23±2.52%; LPB, 7.10±2.99%; BM, 5.23±1.57%; Fig. 1A), suggesting the possibility of LPB as a cell source for the xenograft model. Some samples showed high levels of the LSC population and frequencies of abnormal blasts in PB; however, no significant difference was detected among the three groups (Fig. 1B and data not shown). In contrast, the cell lines K562 and Kasumi-6 displayed low levels of the LSC population (K562, 0.16%; Kasumi-6, 0.02%), whereas 7.72% of the CD34⁺

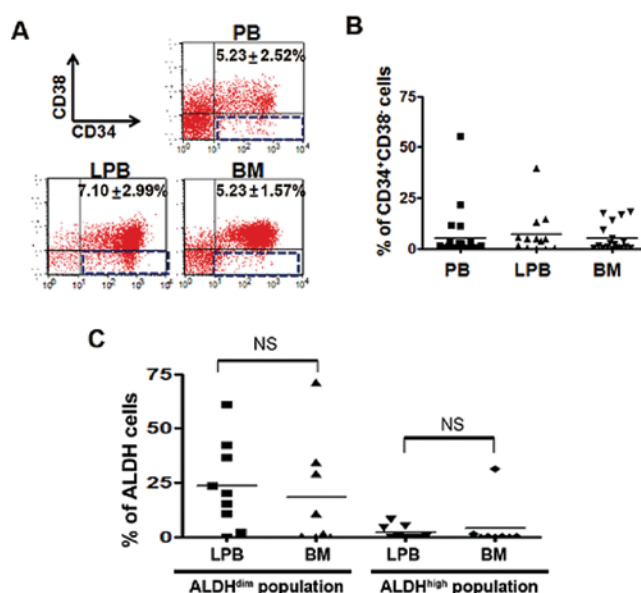


Figure 1. The proportion of CD34⁺CD38⁻ cells and ALDH levels in CD34⁺CD38⁻ cells in AML patient-derived blood samples. (A) Prepared PB, LPB, and BM-MNCs were subjected to FACS analysis. CD34⁺CD38⁻ cells are representative of leukemic stem cells in AML and no significant differences were detected among the three groups. Data shown represent the mean of independent experiments. (B) Statistical analysis of A. (C) Percentage of ALDH^{dim}-expressing cells in CD34⁺CD38⁻ cells prepared from LPB and BM cell samples. There were no significant differences in ALDH^{dim} and ALDH^{high} expression between groups.

cell line, TF-1a, showed a CD34⁺CD38⁻ phenotype (data not shown). Next, we checked the ALDH level in CD34⁺CD38⁻ cells from LPB and BM. As shown in Fig. 1C, no difference in the ALDH^{dim} population was found between the two samples, implying that similar leukemic properties exist between both cell sources in AML. The LSCs of AML patients revealed that the ALDH^{dim} population was higher than the ALDH^{high} population regardless of cell type (ALDH^{dim} population in BM, 18.43%; ALDH^{dim} population in LPB, 23.54%; ALDH^{high}

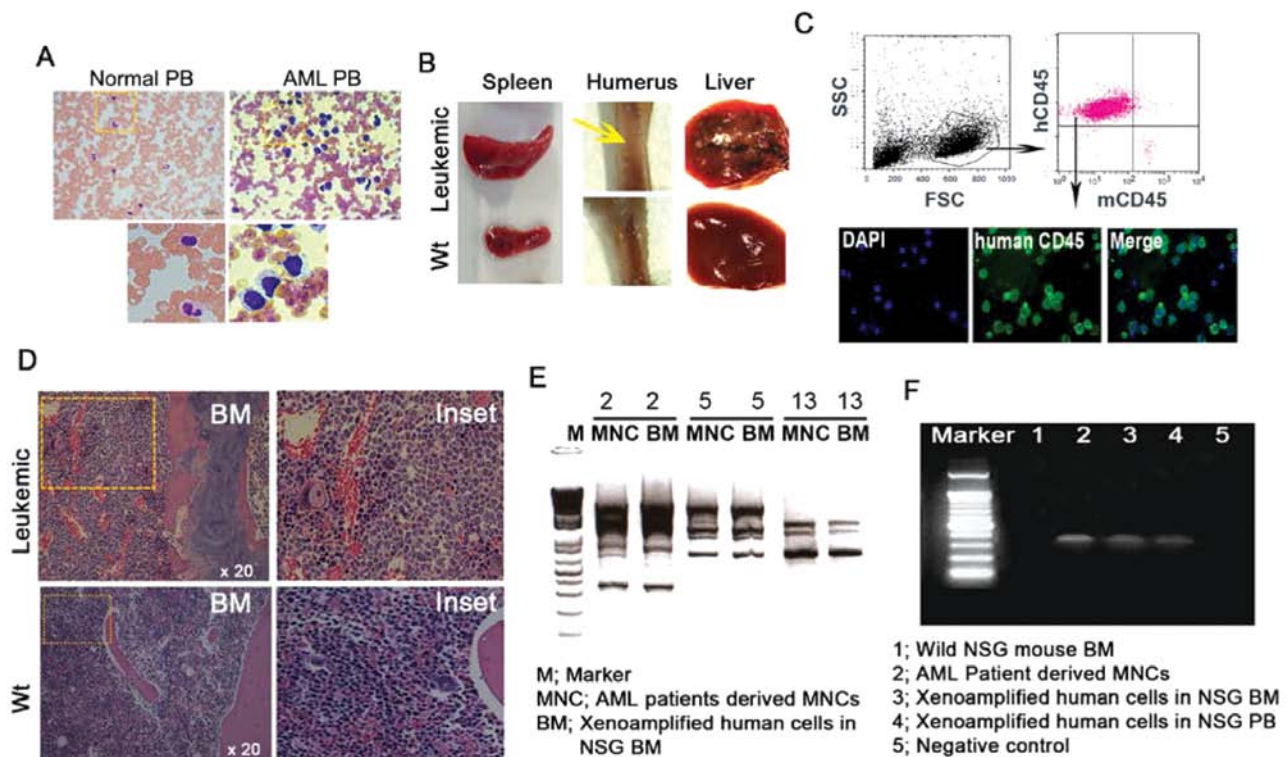


Figure 2. Confirmation of the leukemic xenograft model. (A) Leukapheresed PB showed immature blasts in AML patient blood unlike normal PB. Scale bar, 20 μ m. (B) Gross appearance of leukemic NSG mice. An expanded spleen, suppression of erythropoiesis in BM (yellow arrow), and tumor clusters on the liver were detected in the LPB cell-injected NSG mouse model. (C) High engraftment of human CD45 cells in NSG mouse BM was determined by FACS analysis and microscopic imaging from the samples, which was performed for FACS analysis. (D) H&E staining. Large leukemic xenoamplified human cells are fully located in the BM from the NSG mice compared to high density mouse cells. Enlargements (magnification, x40) are shown in inset images within the main images (magnification, x20). (E) DNA fingerprint PCR. UPF primers of 2, 5, 13 numbers identified the xenoamplified patient cells in the NSG BM cells and primary patient-derived MNCs were of the same origin. (F) Mutation gene PCR. The MLL/AF9 gene was detected in xenoamplified human cells from NSG BM and PB, as well as primary patient-derived MNCs.

population in BM, 4.17%; ALDH^{high} population in LPB, 2.03%; Fig. 1C). These results suggest that the leukemic characteristics, high ALDH^{dim} population and low ALDH^{high} population, in LPB are similar to those observed in BM.

A successful human xenograft model was accompanied by a stable lodgment of injected LPBs. Next, we investigated the engraftment of human cells, gross examination and infiltration of human leukemic cells in leukemic mouse tissues. In the normal humanized mouse model, the mouse model was completed by injecting CD34⁺ cells from normal human cord blood and HSCs; humanized NSG mice displayed normal physiologic condition without virulence (19,20). However, gross appearance from the leukemia humanized mouse clearly showed a significant difference in tumor infiltration when 1×10^7 MNCs from LPB were injected into the NSG mice via the tail vein. First, we checked the existence of AML blasts in patient-derived LPB, and immature blasts were easily detected in the ideal zone from LPB smearing regardless of WHO type (Fig. 2A). In addition, our leukemic xenograft model displayed aberrant and morbid phenomena including liver with disseminating masses, enlarged spleen, and suppression of erythropoiesis in the humerus, suggesting disease induction (Fig. 2B). To confirm human cell infiltration, FACS analysis was carried out on PB and flushed BM. The level of human CD45^{dim} cells in PB from NSG mice at 13 weeks exclusively increased with little existence of murine CD45

cells. Consistently, microscopic imaging also clearly showed FITC-conjugated human CD45 expression in the PB samples, which was performed for FACS analysis (Fig. 2C). BM tissue sections showed immature blasts of human origin with large size and faint hematoxylin staining in vascular regions. The morphology of human cells was easily distinguished from mouse cells in the leukemic mouse BM, and no human cells were found in BM from wild-type mice (Fig. 2D), indicating engraftment of human cells. To confirm whether patient-derived hematopoietic cells can contribute to the leukemic xenograft, DNA fingerprinting and conventional PCR were performed using genomic DNA and specific mutant gene from patient-derived MNCs. DNA fingerprinting allowed the identification of a specific type of individual DNA sequence, known as a 'microsatellite'. LPB from patients who displayed high efficiency of engraftment (93.5%) in BM tissues was used for the DNA fingerprint. As shown in Fig. 2E and F, our data revealed that PCR bands from patient-derived PB-MNCs and BM-MNCs from NSG demonstrated the same pattern of UPF primer of 2, 5, 13 numbers, suggesting patient-derived cells infiltrated the mouse BM (Fig. 2E), and indicated that xenoamplified cells originated from primary MNCs from the AML patients. Leukemic engraftment was monitored by the detection of the MLL/AF9 human mutation gene by PCR. PCR amplifications were positive in primary patient MNCs and xenoamplified human LPB cells in mouse BM and PB (Fig. 2F). Although not all samples readily showed complete

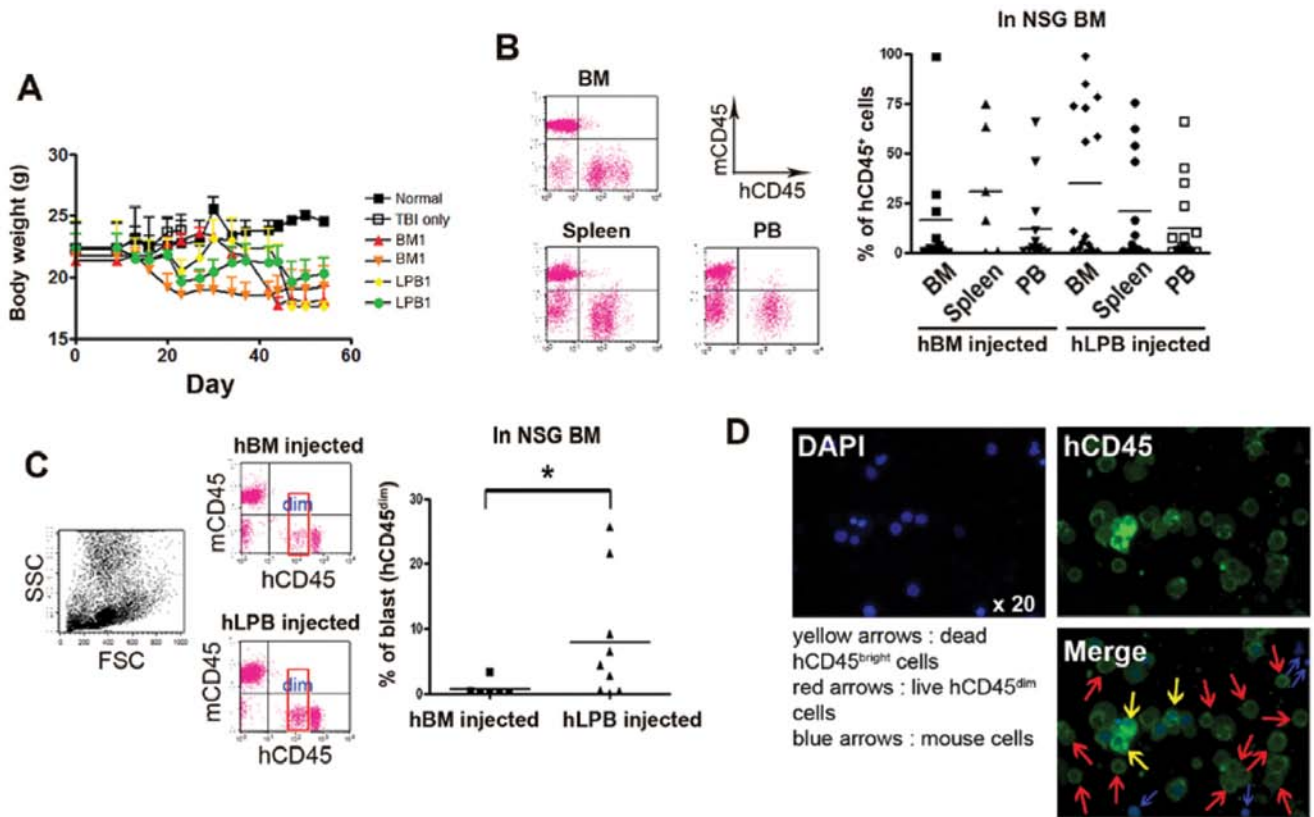


Figure 3. LPB-injected NSG mice showed a high level of CD45^{dim} blasts. (A) Body weight in leukemic cell-injected mice showed significant loss compared to control mice. (B) Stable engraftment of human CD45 cells in various tissues including BM, spleen and PB. There was no difference between the BM cell-injected and LPB cell-injected groups. (C) At 2 weeks, a high level of CD45^{dim} blasts was observed in NSG BM, as shown by FACS analysis. LPB cells were readily grafted into the BM compared to BM cells. (D) Immunocytochemistry of grafted BM cells. hCD45^{high} (yellow arrows) and hCD45^{dim} (red arrows) cells are clearly distinguished by intensity. Only mouse cells without hCD45 are demarcated by blue arrows. DAPI-positive cells indicate dead cells and DAPI-negative cells indicate live cells. Magnification, x20.

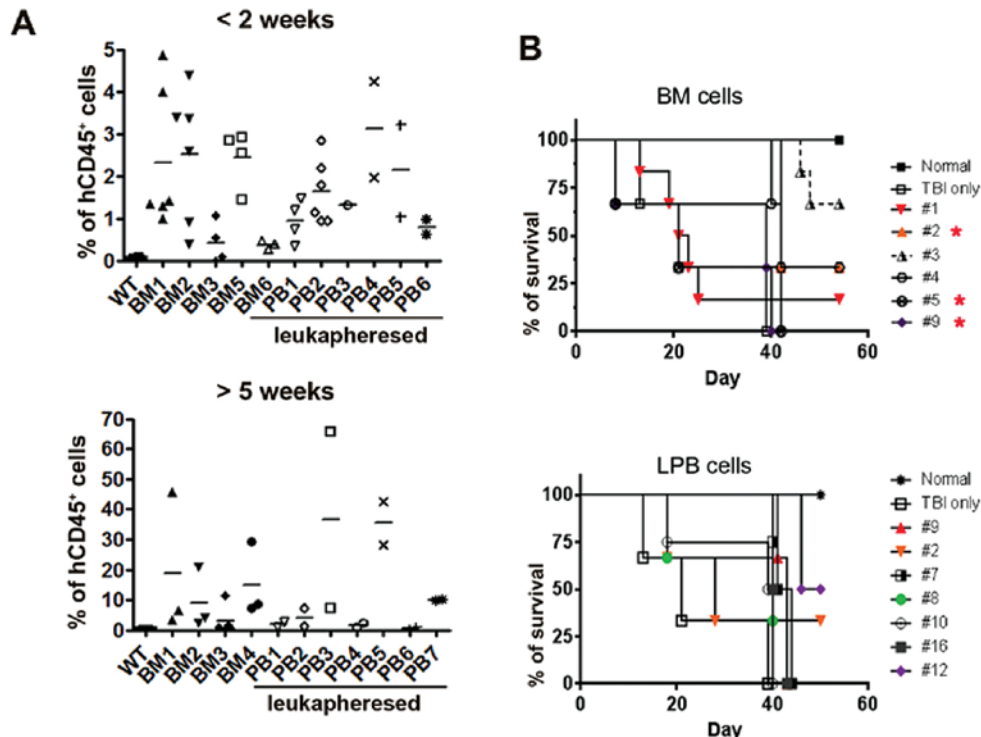


Figure 4. Comparison of human cell engraftment and survival over time. (A) No significant differences during the early time phase and late time phase were detected between the BM cell-injected and LPB cell-injected groups, suggesting LPB cells may be an alternative cell source to BM cells. (B) Within 3 weeks, the LPB cell-injected group displayed stable engraftment with AML blasts and a long life-span.

accordance between the original blood sample and the mouse derived MNCs, most likely due to various factors such as evolution and mutation *in vivo*, we found AML patient-derived cells grafted in the NSG mouse, indicating leukemia manifestation. A xenograft model developed by injecting sorted LSCs can successfully establish advanced leukemia with fewer cell numbers compared to LPB MNCs (data not shown). Without LSC sorting, sufficient numbers of LPB cells can successfully achieve the xenograft model if an adequate number of LSCs are contained in the LPB cell population.

Leukemic xenograft model using LPB cells shows high level of abnormal blasts with CD45^{dim} compared to BM cells. To further investigate whether LPB displays a similar level of engraftment and weight loss compared to BM cells, LPB cells (1×10^7 cells in 200 ml PBS), including functional LSCs, were intravenously (i.v.) injected into NSG mice via the tail vein. As expected, NSG mice, which received two types of cells, BM and LPB, had a similar pattern of weight loss with no significant difference. However, mice receiving patient cells noticeably lost body weight compared to wild-type mice (Fig. 3A). Furthermore, BM, PB and spleens from NSG mice clearly showed high engraftment of CD45⁺ human cells with cancerous symptoms. Because all mice showed increased permissiveness when irradiated before cell transplantation, irradiated female NSG mice were used in the present study (21). Consistently, our data also showed a moderate difference in grafting between irradiated NSG and non-irradiated NSG mice (data not shown). The human CD45 distribution in the BM from NSG mice following the injection of human BM or LPB cells varied (BM cells injected, 0.37 to 99.04%; LPB cells injected, 0.09 to 99.05%). In PB and spleen, the number of human BM or LPB cells also varied (in PB: BM cells injected, 0.27 to 65.68%; LPB cells injected, 0.01 to 65.80%; in spleen: BM cells injected, 0.43 to 74.49%; LPB cells injected, 0.26 to 75.47%). Although no significant difference in BM engraftment was found between the BM- and LPB-injected groups, the LPB-injected group revealed a slightly higher average engraftment when LPB cells were injected into NSG mice compared to mice that received BM cells (LPB cells injected into NSG BM, $34.9 \pm 9.39\%$; BM cells injected into NSG BM, $16.56 \pm 9.68\%$; Fig. 3B). Mice were sacrificed and xenoamplified leukemic cells were harvested from the tissues when signs of sickness became evident or the hCD45 in PB exceeded 70% during the time from 2 to 11 weeks post-injection. We then examined the percentage of human CD45^{dim} abnormal blasts in BM tissues. As AML blasts show a dim intensity of staining with the leukocyte common antigen CD45 antibody, CD45 has been used to distinguish AML cells from normal white blood cells (22). FACS data certainly showed a high engraftment of abnormal blasts in NSG mouse BM 2 weeks after LPB cells were injected (Fig. 3C). BM cell-injected mice displayed a significantly low CD45^{dim} cell population in the BM compared to the LPB cell-injected mice (Fig. 3C). The intensity of human CD45 cells in gated cells was divided into two fractions, a 'dim' and a 'high' population. Notably, human CD45^{dim} cells in the LPB-injected NSG mice were clearly distinguished from CD45^{high} cells (Fig. 3B and C). We only counted the 'dim' population of CD45-positive cells to calculate abnormal cells. Moreover, fluorescence microscopic images also showed that

CD45^{high} cells and CD45^{dim} cells were distinguishable in the BM cells. A small nucleus without the human CD45 marker identified mouse cells and DAPI-positive dead human CD45^{high} and live human CD45^{dim} cells were present in the BM flushed cells (Fig. 3D). Surprisingly, three LPB samples, which showed above average expression of ALDH^{dim} and LSCs, had a significant increase in fold change of CD45^{dim} cells in NSG BM at 2 weeks post-transplantation, as well as high engraftment in the NSG mice (Fig. 1A and C and Fig. 3C). We found that human cell engraftment fully relied on individual variations and was dependent on whether a high level of ALDH^{dim}-expressing LSCs was present or not. The strength of LPB as a cell source in the leukemic xenograft mouse model was apparent when ALDH^{dim}-expressing LSCs were selected.

Leukemic xenograft model using LPB cells displays longevity with stable engraftment. In general, leukemic xenograft mouse models have been used to study biological features in leukemia and to investigate responses to antitumor drugs. Therefore, to maintain the longevity of a mouse with cancer is one important factor by which to elicit experimental results *in vivo*. Unfortunately, since it is not acceptable to acquire huge amounts of leukemic stem cells from patient BM, many *in vivo* studies using leukemic xenograft models are defeated before the start of the experiment, or have difficulty acquiring consistent data interpretation due to individual diversity. Therefore, we also addressed the differential efficacy of human cell lodgment in a time-dependent manner with longevity. Time was divided into an early time phase (<2 weeks) and a late time phase (>5 weeks). From 3 to 9 heads of mice were used for each sample. Lodgment of human CD45 cells in BM was not significantly different between BM and LPB cell sources in a time phase manner (Fig. 4A). CD45-positive cells in the early time phase were fewer in number than that observed in the late time phase, and CD45-positive cells gradually increased in a time-dependent manner for both primary human samples studied, BM and LPB. Next, we sought to address the stable longevity of abnormal blasts in engrafted mice. Three to 6 heads of mice that received human BM cells, and 2 to 4 heads of mice which received human LPB cells, were used to examine they longevity. Although unexpected mortality was monitored in the BM cell-injected NSG mice due to individual characteristics, we found that BM and LPB cells that were grafted into NSG mice in the presence of abnormal blasts continuously maintained a stable survival at >50% until 8 weeks post-injection. Mice injected with LPB cells showed low mortality (Fig. 4B), suggesting that LPB may maintain the model for a longer time in which to examine the *in vivo* study.

Discussion

Xenograft models using human AML cells are important tools by which to study the pathophysiology of AML, including the tumor microenvironment, leukemic stem cells and drug resistance, *in vivo*. Moreover, advanced xenograft models help to screen individualized molecular treatment modalities *in vivo*. AML is a stem cell-mediated disease, and a variable population of LSCs has been associated with the disease. Therefore, we hypothesized that LPB may be a preferable cell

source to generate the xenograft model if the frequency of ALDH^{dim}-expressing LSCs is high. Similarly, BM cells from AML patients are considered to be a superior cell source due to its high level of LSCs compared to PB cells. However, an important limitation of BM is that it can only be obtained in small volumes from patients. Because a synchronized mouse model prepared from a single sample without variation has yielded reproducible data in disease biology, we attempted to accumulate evidence from this limited experiment, which can contribute towards completing the human xenograft model using LPB cells. The leukemic xenograft model is also hampered by individual patient variation and the short life-span of immunodeficient mice. A large amount of material from the same patient can minimize these deficits. In addition, the leukemic xenograft model using LPB cells shows no significant difference in graft and cell amplification with genetic abnormalities when compared to the model using BM cells. LPB is also capable of producing numerous models at one time. Importantly, LPB cells can support a longer life-span without sudden death, and can maintain more than 60% survival 5 weeks after human AML cell injection. We cannot exclude that BM cells may aggressively progress with AML features and graft-versus-host disease induction by co-infused T cells in the graft (23). The use of LPB cells prevents high mortality. Consistent with previous reports, stem cell quantity and quality of LPB appeared to vary and was difficult to estimate among patients (24). Some patients have more than sufficient stem cells in LPB, while others do not. The frequency of LSCs in LPB cells depends on multiple parameters, such as mobilization timing, chemotherapy type, and cytokine addition. Because a variety of reasons affect the status of circulating blood cells, it is difficult to determine the best sample without a proper indicator in the xenograft model. To overcome the frailty of reproducibility and volume, some investigators have used leukemic cell lines, such as TF-1a and K562, instead of primary AML cells (25-27). However, leukemic cell lines are fundamentally different from primary leukemic cells in grafting. Our data also revealed low efficacy of the CD34⁺ cell line TF-1a with at least a 2- to 3-fold reduction in grafting compared to that of primary cells (data not shown). To develop a more reasonable protocol with which to produce a xenograft model, our results suggest using LPB with high levels of ALDH^{dim}-expressing LSCs. Moreover, one of the advantages of LPB is that the sample naturally occurs during the course of treatment. Blood collection does not require anesthesia or antibiotic treatment. We also demonstrated the potential of LPB as an advantageous cell source with which to generate a xenograft model with a long life-span. Progenitor cells from LPB displayed rapid hematopoietic recovery after conditioning regimens with high dose therapy (28). This rapid recovery may reduce mortality and morbidity. Xenograft models are also very diverse in many factors, including recipient permissiveness, age and gender (21). Ultimately, the goal of xenograft models is to be clinically relevant, mimic the situation of the patients and be sufficient to perform a wide spectrum of experiments. Depending on these goals, we found that human LPB is a beneficial cell source for a xenograft model to satisfy the patient setting. To our knowledge, this direct comparison between using BM and LPB cells in a leukemic xenograft model has not been previously reported. We compared the effi-

ciency of both BM and LPB cell engraftment using NSG mice and retrospectively found that ALDH^{dim}-expressing LSCs may belong in the category of cells which can induce a successful graft model. Our data are informative in deciding which cell sources to use to accomplish a successful xenograft model. A xenograft model with stable leukemic properties is necessary to determine the effects of antitumor drugs and immune cell therapies, such as those using cytotoxic T cells and natural killer cells.

In conclusion, LPB cells, which contain high levels of ALDH^{dim}-expressing CD34⁺CD38⁻ cells, can serve as a suitable alternative cell source to BM cells for the generation of leukemic xenograft models.

Acknowledgements

This research was partly supported by a grant from the National R&D Program for Cancer Control, Ministry for Health and Welfare, Republic of Korea (1020370).

References

- Gopinathan A and Tuveson DA: The use of GEM models for experimental cancer therapeutics. *Dis Model Mech* 1: 83-86, 2012.
- Richmond A and Su Y: Mouse xenograft models vs GEM models for human cancer therapeutics. *Dis Model Mech* 1: 78-82, 2008.
- Kelland LR: Of mice and men: values and liabilities of the athymic nude mouse model in anticancer drug development. *Eur J Cancer* 40: 827-836, 2004.
- McCune JM, Namikawa R, Kaneshima H, Shultz LD, Lieberman M and Weissman IL: The SCID-hu mouse: murine model for the analysis of human hematolymphoid differentiation and function. *Science* 241: 1632-1639, 1988.
- Mosier DE, Gulizia RJ, Baird SM and Wilson DB: Transfer of a functional human immune system to mice with severe combined immunodeficiency. *Nature* 335: 256-259, 1988.
- Lubin I, Faktorowich Y, Lapidot T, Gan Y, Eshhar Z, Gazit E, *et al*: Engraftment and development of human T and B cells in mice after bone marrow transplantation. *Science* 252: 427-431, 1991.
- Lapidot T, Pflumio F, Doedens M, Murdoch B, Williams DE and Dick JE: Cytokine stimulation of multilineage hematopoiesis from immature human cells engrafted in SCID mice. *Science* 255: 1137-1141, 1992.
- Cheung AM, Wan TS, Leung JC, Chan LY, Huang H, Kwong YL, *et al*: Aldehyde dehydrogenase activity in leukemic blasts defines a subgroup of acute myeloid leukemia with adverse prognosis and superior NOD/SCID engrafting potential. *Leukemia* 21: 1423-1430, 2007.
- Ishikawa F, Yasukawa M, Lyons B, Yoshida S, Miyamoto T, Yoshimoto G, *et al*: Development of functional human blood and immune systems in NOD/SCID/IL2 receptor {gamma} chain(null) mice. *Blood* 106: 1565-1573, 2005.
- Ishikawa F, Yoshida S, Saito Y, Hijikata A, Kitamura H, Tanaka S, *et al*: Chemotherapy-resistant human AML stem cells home to and engraft within the bone-marrow endosteal region. *Nat Biotechnol* 25: 1315-1321, 2007.
- Will B, Kawahara M, Luciano JP, Bruns I, Parekh S, Erickson-Miller CL, *et al*: Effect of the nonpeptide thrombopoietin receptor agonist Eltrombopag on bone marrow cells from patients with acute myeloid leukemia and myelodysplastic syndrome. *Blood* 114: 3899-3908, 2009.
- Sanchez PV, Perry RL, Sarry JE, Perl AE, Murphy K, Swider CR, *et al*: A robust xenotransplantation model for acute myeloid leukemia. *Leukemia* 23: 2109-2117, 2009.
- Goardon N, Marchi E, Atzberger A, Quek L, Schuh A, Soneji S, *et al*: Coexistence of LMPP-like and GMP-like leukemia stem cells in acute myeloid leukemia. *Cancer Cell* 19: 138-152, 2011.
- Lapidot T, Sirard C, Vormoor J, Murdoch B, Hoang T, Caceres-Cortes J, *et al*: A cell initiating human acute myeloid leukaemia after transplantation into SCID mice. *Nature* 367: 645-648, 1994.

15. Sarry JE, Murphy K, Perry R, Sanchez PV, Secretto A, Keefer C, *et al*: Human acute myelogenous leukemia stem cells are rare and heterogeneous when assayed in NOD/SCID/IL2R γ c-deficient mice. *J Clin Invest* 121: 384-395, 2011.
16. Gerber JM, Smith BD, Ngwang B, Zhang H, Vala MS, Morsberger L, *et al*: A clinically relevant population of leukemic CD34(+)/CD38(-) cells in acute myeloid leukemia. *Blood* 119: 3571-3577, 2012.
17. Hong SH, Nah HY, Lee JY, Lee YJ, Lee JW, Gye MC, *et al*: Estrogen regulates the expression of the small proline-rich 2 gene family in the mouse uterus. *Mol Cells* 17: 477-484, 2004.
18. Lee JY, Park C, Cho YP, Lee E, Kim H, Kim P, *et al*: Podoplanin-expressing cells derived from bone marrow play a crucial role in postnatal lymphatic neovascularization. *Circulation* 122: 1413-1425, 2010.
19. Shultz LD, Ishikawa F and Greiner DL: Humanized mice in translational biomedical research. *Nat Rev Immunol* 7: 118-130, 2007.
20. Choi B, Chun E, Kim M, Kim SY, Kim ST, Yoon K, *et al*: Human T cell development in the liver of humanized NOD/SCID/IL-2R γ (null)(NSG) mice generated by intrahepatic injection of CD34(+) human (h) cord blood (CB) cells. *Clin Immunol* 139: 321-335, 2011.
21. Notta F, Doulatov S and Dick JE: Engraftment of human hematopoietic stem cells is more efficient in female NOD/SCID/IL-2R γ -null recipients. *Blood* 115: 3704-3707, 2010.
22. Lacombe F, Durrieu F, Briaux A, Dumain P, Belloc F, Bascans E, *et al*: Flow cytometry CD45 gating for immunophenotyping of acute myeloid leukemia. *Leukemia* 11: 1878-1886, 1997.
23. Whartenby KA, Straley EE, Kim H, Racke F, Tanavde V, Gorski KS, *et al*: Transduction of donor hematopoietic stem-progenitor cells with Fas ligand enhanced short-term engraftment in a murine model of allogeneic bone marrow transplantation. *Blood* 100: 3147-3154, 2002.
24. Breems DA, van Hennik PB, Kusadasi N, Boudewijn A, Cornelissen JJ, Sonneveld P and Ploemacher RE: Individual stem cell quality in leukapheresis products is related to the number of mobilized stem cells. *Blood* 87: 5370-5378, 1996.
25. Zhang J, Yang WH, Yang XD, Shi ZX, Wang XL, Yu WJ, *et al*: Establishment and identification of CML model via injection of K562 cells into the murine caudal vein. *Zhongguo Shi Yan Xue Ye Xue Za Zhi* 20: 773-776, 2012 (In Chinese).
26. Park J, Kim KI, Koh Y, Won NH, Oh JM, Lee DS, *et al*: Establishment of a new Glivec-resistant chronic myeloid leukemia cell line, SNUCML-02, using an in vivo model. *Exp Hematol* 38: 773-781, 2010.
27. Lee J, Li M, Milwid J, Dunham J, Vinegoni C, Gorbator R, *et al*: Implantable microenvironments to attract hematopoietic stem/cancer cells. *Proc Natl Acad Sci USA* 109: 19638-19643, 2012.
28. Elias AD, Ayash L, Anderson KC, Hunt M, Wheeler C, Schwartz G, *et al*: Mobilization of peripheral blood progenitor cells by chemotherapy and granulocyte-macrophage colony-stimulating factor for hematologic support after high-dose intensification for breast cancer. *Blood* 79: 3036-3044, 1992.